RESEARCH ARTICLE

NMR IN BIOMEDICINE WILEY

Multiparametric renal magnetic resonance imaging: A reproducibility study in renal allografts with stable function

Rebeca Echeverria-Chasco[1,2] | Paloma L. Martin-Moreno[2,3] |
Nuria Garcia-Fernandez[2,3] | Marta Vidorreta[4] | Verónica Aramendia-Vidaurreta[1,2] |
David Cano[1] | Arantxa Villanueva[2,5] | Gorka Bastarrika[1,2] |
Maria A. Fernández-Seara[1,2]

[1]Department of Radiology, Clínica Universidad de Navarra, Pamplona, Spain

[2]IdiSNA, Instituto de Investigación Sanitaria de Navarra, Pamplona, Spain

[3]Department of Nephrology, Clínica Universidad de Navarra, Pamplona, Spain

[4]Siemens Healthcare, Madrid, Spain

[5]Electrical Electronics and Communications Engineering Department and Smart Cities Institute, Public University of Navarre, Pamplona, Spain

Correspondence
Nuria Garcia-Fernandez, Department of Nephrology, Clínica Universidad de Navarra, Pio XII, 36, 31008, Pamplona, Spain.
Email: nrgarcia@unav.es

Funding information
Government of Navarra; Grant Number: PC181-182 RM-RENAL
Rebeca Echeverria-Chasco received Ph.D. grant support from Siemens Healthcare Spain

Monitoring renal allograft function after transplantation is key for the early detection of allograft impairment, which in turn can contribute to preventing the loss of the allograft. Multiparametric renal MRI (mpMRI) is a promising noninvasive technique to assess and characterize renal physiopathology; however, few studies have employed mpMRI in renal allografts with stable function (maintained function over a long time period). The purposes of the current study were to evaluate the reproducibility of mpMRI in transplant patients and to characterize normal values of the measured parameters, and to estimate the labeling efficiency of Pseudo-Continuous Arterial Spin Labeling (PCASL) in the infrarenal aorta using numerical simulations considering experimental measurements of aortic blood flow profiles. The subjects were 20 transplant patients with stable kidney function, maintained over 1 year. The MRI protocol consisted of PCASL, intravoxel incoherent motion, and T1 inversion recovery. Phase contrast was used to measure aortic blood flow. Renal blood flow (RBF), diffusion coefficient (D), pseudo-diffusion coefficient (D*), flowing fraction (*f*), and T1 maps were calculated and mean values were measured in the cortex and medulla. The labeling efficiency of PCASL was estimated from simulation of Bloch equations. Reproducibility was assessed with the within-subject coefficient of variation, intraclass correlation coefficient, and Bland-Altman analysis. Correlations were evaluated using the Pearson correlation coefficient. The significance level was *p* less than 0.05. Cortical reproducibility was very good for T1, D, and RBF, moderate for *f*, and low for D*, while medullary reproducibility was good for T1 and D. Significant correlations in the cortex between RBF and *f* (r = 0.66), RBF and eGFR (r = 0.64), and D* and eGFR (r = −0.57) were found. Normal values of the measured parameters

---

Abbreviations used: ASL, arterial spin labeling; BOLD, blood oxygenation level-dependent; BS, background suppression; BW, bandwidth; CKD, chronic kidney disease; CV_{ws}, within subject coefficient of variation; DWI, diffusion-weighted imaging; ECG, electrocardiogram; eGFR, estimated glomerular filtration rate; FA, flip angle; FOCI, Frequency Offset Corrected Inversion; FOV, field of view; GFR, glomerular filtration rate; GRAPPA, Generalized Autocalibrating Partial Parallel Acquisition; HASTE, half-Fourier-acquired single-shot turbo spin echo; ICC, intraclass correlation coefficient; IR, inversion recovery; IVIM, intravoxel incoherent motion; mpMRI, multiparametric MRI; PCA, principal component analysis; PCASL, Pseudo Continuous Arterial Spin Labeling; PLD, postlabeling delay; PWI, perfusion-weighted image; RBF, renal blood flow; ROI, region of interest; SD, standard deviation; SE-EPI, spin-echo echo planar imaging; SNR, signal-to-noise ratio; tSNR, temporal signal-to-noise ratio; TI, inversion time; TR, repetition time; VENC, encoding velocity.

---

employing the mpMRI protocol in kidney transplant patients with stable function were characterized and the results showed good reproducibility of the techniques.

KEYWORDS

arterial spin labeling, intravoxel incoherent motion, kidney transplant, multiparametric MRI, reproducibility, T1 mapping

1 | INTRODUCTION

Chronic kidney disease (CKD) is a major global social problem with an estimated prevalence of 13.4%.[1] Approximately 7.4 million people are affected by kidney failure.[2] The treatment of choice for these patients is kidney transplantation. After transplantation, monitoring renal allograft function is key for the early detection of allograft impairment and thus to evaluate the appropriate therapeutic strategies to prevent allograft loss.

Kidney allograft function can be assessed by measuring the glomerular filtration rate (GFR). However, measurement of the GFR using a filtration marker such as inulin, iothalamate, or iohexol, although considered the gold standard, is time consuming and onerous for the patient and thus is not used in clinical practice. Instead, guidelines for monitoring kidney allograft function recommend measuring serum creatinine for estimating the glomerular filtration rate (eGFR) using an equation.[3] However, there is poor agreement between eGFR and measured GFR in renal transplant recipients. In addition, eGFR has poor reliability for monitoring kidney function over time in this population.[4] Imaging methods that are currently employed in the clinical routine have significant limitations,[5,6] and they are neither adequate to detect early renal dysfunction, nor to predict the disease progression of the allograft.

Multiparametric renal MRI has emerged as a promising noninvasive technique for the assessment and characterization of both renal physiology and physiopathology that has the potential to overcome the current problems. A growing number of groups are investigating its feasibility and initial results show that this technique provides quantitative measurements of potential renal biomarkers associated with different pathological processes that are important in the allograft evolution. Multiparametric MRI (mpMRI) generally refers to protocols that include different pulse sequences that image some of these biomarkers, with the choice of sequences depending on the study's specific aims. These biomarkers are sensitive to variations in tissue perfusion, oxygenation, or microstructure (including inflammation and fibrosis).[7]

Several studies have combined diffusion and perfusion sequences. For example, Heusch et al.[8] were able to demonstrate a correlation between renal allograft perfusion measured with arterial spin labeling (ASL) and the flowing fraction estimated with intravoxel incoherent motion (IVIM), and they also reported correlations of both parameters with serum creatinine levels and eGFR in a group of 17 renal transplant patients. When comparing allografts with impaired function early after transplantation to allografts with normal function and healthy controls, Ren et al.[9] reported a reduction of diffusion and perfusion parameters in allografts with impaired function and showed that the combination of IVIM and ASL improved the diagnostic value of the protocol compared with each technique alone. Bane et al.[10] employed a mpMRI protocol including diffusion, blood oxygenation level-dependent (BOLD), and T1 mapping to evaluate the allograft in kidney transplant patients in both those with stable function and in those with chronic dysfunction. Their results revealed the diagnostic potential of combining diffusion parameters and T1 to detect chronic dysfunction with established fibrosis and to predict eGFR decline at 18 months. They also reported good reproducibility of mpMRI parameters, although it was only assessed in a small group of four patients. T1 and T2 values were measured in combination with diffusion by Adams et al.,[11] who reported an increase in T1 and T2 after transplantation, especially in early transplants, and a decrease in diffusion parameters, compared with healthy controls. T1 correlated best with eGFR in addition to emerging as a significant predictor of interstitial fibrosis.

However, few studies have been reported using mpMRI in renal allografts with stable function maintained over a long time period. This group of patients offers the opportunity to determine the range of normal values of mpMRI parameters against which measurements obtained in patients with suspected dysfunction can be compared. Thus the aims of this work were to assess the reproducibility of performing multiparametric MRI and to characterize normal values of the measured parameters in this group of patients.

The number of sequences included in the multiparametric protocol determines the duration of the MRI examination. In this study, the protocol was designed to restrict the examination duration to 30 min, reducing the burden on the patient. Thus, considering the potential utility of the MRI parameters found in previous studies, three sequences were included, namely, ASL, IVIM, and T1 mapping.

ASL evaluates tissue perfusion without exogenous contrast agents by employing magnetically labeled arterial blood water as endogenous tracer, enabling the quantification of renal blood flow (RBF) in physiological units of ml/min/100 g of tissue.[12] IVIM estimates both slow diffusion in the tissue and fast molecular movement associated with blood microcirculation and tubular flow, by applying a range of low amplitude diffusion gradients (i.e., b-values < 200 s/mm^2), in addition to the b-values used in conventional diffusion-weighted imaging (DWI).[13] The IVIM model can separate both signal contributions by fitting a bi-exponential decay. One of the most common strategies with which to estimate T1 is the inversion recovery (IR) technique.[14] This strategy employs a 180° pulse to invert the longitudinal magnetization, acquiring the image after an inversion time (TI). This procedure is repeated several times with varying TI to sample the longitudinal relaxation curve and subsequently fit the data to the T1 model.

None of these sequences use contrast agents, which in renal patients is considered especially advantageous, as administration of gadolinium-based contrast agents could be contraindicated,[15] because they have been associated with the development of nephrogenic systemic fibrosis. Moreover, reports of gadolinium deposition in the brain have raised new concerns over their safety.

2 | MATERIALS AND METHODS

2.1 | Subjects

The study was approved by the local Ethics Research Committee of the University of Navarra. Written informed consent was obtained from all subjects. The inclusion criteria were: patients older than 18 years, undergoing a transplant more than 1 year before the start of the study, with an eGFR of more than 50 ml/min/1.73m^2 and stable throughout the last year (i.e., serum creatinine levels varied by ≤ 0.2 mg/dl during the last year and no events changed their clinical status during the study). The general exclusion criterion was subjects with contraindications for MRI. Patients were recruited by their referring nephrologist.

2.2 | Reproducibility study

From January 2020 to August 2021, 20 subjects participated in this study. All patients were scanned in two MRI sessions on separate days at least 1 week apart to assess intervisit reproducibility. These examinations are referred to as Exam 1 and Exam 2 in the text and figures. No specific preparations, such as fasting or fluid intake restriction, were undertaken before the MR examinations; however the MR examinations were scheduled at the same time on both days.

All participants underwent clinical laboratory measurements of urine and blood samples, including serum creatinine. In eight patients, the samples were collected on the day prior to the first MRI examination, whereas in the others, sample collection was carried out between 1 week and 3 months prior to the study. In patients in which the time between the two MRI examinations was longer than 3 months, measurements of serum creatinine were also obtained prior to the second examination. eGFR was calculated according to the Chronic Kidney Disease Epidemiology Collaboration (CKD-EPI) equation based on creatinine.[16]

2.3 | MRI protocol

MR examinations were performed on a 3.0-T Siemens Skyra scanner (Siemens Healthcare GmbH, Erlangen, Germany) using a 32-channel spine coil integrated in the scanner table and an 18-channel flexible body array coil.

First, localizers and anatomical images were acquired during breath-holds using a T2-weighted half-Fourier-acquired single-shot turbo spin echo (HASTE) sequence in coronal orientation and a T1-weighted volumetric interpolated breath-hold examination (VIBE) sequence in axial orientation. In addition, specific localizers to visualize the aorta were also acquired. Anatomical images and localizers enabled accurate positioning of the imaging planes and labeling plane in the ASL sequence.

As previously mentioned, the protocol consisted of ASL, IVIM, and T1 mapping. The images were acquired at the same geometrical position in coronal-oblique or sagittal-oblique orientation, centered in the transplanted kidney. Because the allograft is placed in the iliac fossa under different orientations, orienting the imaging slab along the long axis of the kidney was not always possible. Three slices were acquired in each of the sequences. In the second MR examination, the imaging planes of the first study were taken as reference, as well as the location and orientation of the labeling plane in ASL, to match the locations between both scans. All images were acquired in free breathing. The duration of a complete examination was 30 min.

In addition, a phase contrast (PC) sequence was run in one of the two examinations (depending on the time available) to characterize the blood velocity profile in the abdominal aorta, with the aim of evaluating the labeling efficiency by simulations. Imaging parameters for all sequences are detailed below.

2.3.1 | Arterial spin labeling

Tissue perfusion was evaluated using a Pseudo-Continuous Arterial Spin Labeling (PCASL) sequence with a spin-echo echo planar imaging (SE-EPI) readout, following published consensus recommendations.[12]

The PCASL labeling plane was located approximately 8 cm above the center of the kidney, perpendicular to the aorta. The labeling was implemented with a train of short Hann-shaped radiofrequency pulses with a duration of 500 μs, a period of 1 ms, and a flip-angle (FA) of 24.6°,

resulting in a B1$_{average}$ of 1.6 μT. The total labeling duration (τ) was 1.6 s. PCASL was unbalanced with a labeling average gradient (G$_{ave}$) strength of 0.5 mT/m and slice-selective to average gradient ratio (G$_{max}$/G$_{ave}$ ratio) of 6. This strategy of lowering the average gradient and G$_{max}$/G$_{ave}$ ratio was previously reported to increase the labeling robustness to field inhomogeneities and pulsatile flow in the aorta.[17]

Presaturation pulses selective to the imaging slices were applied at the beginning of the PCASL sequence to saturate the in-plane signal. Background suppression (BS)[18] pulses were employed to suppress the background tissue signal for a range of T1s of 1000–2500 ms. BS was implemented using a selective inversion Frequency Offset Corrected Inversion (FOCI) pulse prior to labeling, followed by two nonselective FOCI pulses after the labeling. The postlabeling delay (PLD) was 1.2 s. An M0 image, in which presaturation, BS, and ASL labeling pulses were not employed, was acquired at the beginning of the ASL sequence, followed by 25 pairs of control-label images.

The readout parameters were slice thickness = 5 mm (gap = 2.5 mm), acquisition matrix = 96 x 96, field of view (FOV) = 288 x 288 mm², repetition time (TR) = 5000 ms, echo time (TE) = 23 ms, Generalized Autocalibrating Partial Parallel Acquisition (GRAPPA) factor 2, 6/8 partial Fourier, bandwidth (BW) = 1890 Hz/pixel, and phase oversampling = 25%. Fat-suppression pulses were employed before the excitation pulses for each slice. The acquisition time was 4.5 min.

2.3.2 | Phase contrast to assess labeling efficiency

Blood flow velocity profiles were characterized for blood spins flowing through the PCASL labeling plane using a PC sequence. Therefore, the imaging plane had the same translation and rotation as the PCASL labeling plane. A retrospectively ECG-triggered acquisition was employed during a single breath-hold, with through plane-encoding direction and an encoding velocity (V_{enc}) of 150 cm/s.

The PC-MRI parameters were TR = 31.2 ms, TE = 2.89 ms, FA = 20°, FOV = 332.8 x 206.3 mm², slice thickness = 5 mm, acquisition matrix = 256 x 160, BW = 455 Hz/pixel, partial Fourier = 7/8, GRAPPA factor = 2, and 50 reconstructed cardiac phases.

2.3.3 | Intravoxel incoherent motion

Tissue diffusion and pseudo-diffusion were assessed using IVIM with a single-shot EPI readout. The IVIM sequence was configured according to consensus recommendations on renal diffusion.[13]

To separate the contribution of flow from pure diffusion, 13 b-values ranging from 0 to 800 s/mm² were used: 0, 5, 10, 20, 30, 50, 70, 100, 200, 300, 400, 500, and 800 s/mm². Eight low b-values were included to better characterize the fast signal decay. Monopolar gradients were applied in three orthogonal directions (three repetitions each) and acquisitions were subsequently averaged to minimize the effects of diffusion anisotropy.

The readout parameters were slice thickness = 5 (gap = 2.5) mm, acquisition matrix = 128 x 128, FOV = 288 x 288 mm², TR/TE = 5000/84 ms, GRAPPA factor = 2, BW = 1890 Hz/pixel, and phase oversampling = 25%. Fat-suppression (SPAIR) pulses were employed. The acquisition time was 9 min.

2.3.4 | T1 mapping

To measure the longitudinal relaxation time of kidney tissue, an IR sequence with an SE-EPI readout was employed, with 14 inversion times—200, 300, 400, 500, 600, 700, 800, 900, 1000, 1200, 1400, 1600, 1800, and 2000 ms—and TR = 5 s, following published consensus recommendations.[14] The readout parameters were identical to those for the PCASL-SE-EPI sequence. The acquisition time was 1.5 min.

2.4 | Image processing

Image processing was performed using custom scripts in MATLAB (MathWorks).

2.4.1 | Motion correction

Motion was corrected using a group-wise registration method based on principal component analysis[19] implemented in Elastix,[20] grouping the data into two sets of images according to their image resolution: Set 1: M0, ASL label and control pairs and T1 images; and Set 2: IVIM images.

2.4.2 | Renal blood flow quantification

PCASL control and label images were subtracted and averaged after discarding outliers, and perfusion-weighted images (PWIs) were calculated by normalizing voxel-wise the perfusion signal with the M0 signal. Outliers were discarded if the signal in the cortical region of interest (ROI) (see Section 2.4.6 for further details) was higher or lower than mean ± 2 standard deviation (SD). Temporal signal-to-noise ratio (TSNR) was calculated as the ratio between the time-averaged perfusion signal across all repetitions (including outliers) and the temporal SD.

RBF maps were computed using the single compartment model (Equation (1)).[12]

$$RBF(ml/min/100g) = PWI \frac{6000\lambda}{2\alpha T1_b} \frac{e^{\frac{PLD}{T1_b}}}{1 - e^{\frac{\tau}{T1_b}}}, \tag{1}$$

where $\alpha = 0.65$ is the labeling efficiency, considering the PCASL efficiency as 0.75 (see the Results section for further details) and the effect of the two BS pulses, $\lambda = 0.9$ ml/g is the tissue-blood water partition coefficient, and $T1_b = 1.65$ s is the arterial blood longitudinal relaxation time.

2.4.3 | Blood velocity profile and labeling efficiency estimation

For this analysis, data from six patients were excluded because of ECG triggering errors. Therefore, aortic blood flow velocity profiles were obtained for 12 patients, who were divided into two groups according to their ages (because of the known effect of age on blood flow velocity[21]): Group 1 contained patients younger than 50 years and Group 2 consisted of those aged 50 years or older.

Blood velocity maps were calculated as $v = \Delta\emptyset V_{enc}/\pi$, where $\Delta\emptyset$ is the measured phase variation. The aorta was segmented automatically in each of the magnitude images according to a previously described procedure[17] and the segmented ROI was applied to the velocity maps. Peak and average velocities within the ROI were extracted. Group average velocity waveforms were computed. Differences in systolic peak velocity between groups 1 and 2 were evaluated using a Mann-Whitney-Wilcoxon test.

To estimate the labeling efficiency of PCASL, the evolution of the longitudinal magnetization of the aortic blood spins crossing the labeling plane was simulated based on Bloch equations[22] for the measured range of velocities and considering off-resonance frequencies in the 0–500 Hz interval. Inversion efficiency maps were generated as previously reported for each group.[17]

2.4.4 | IVIM parameter maps quantification

IVIM parameter maps were generated by fitting a bi-exponential model to the signal intensity decay (Equation (2)).[13]

$$S_b = fS_0 e^{-bD^*} + (1-f)S_0 e^{-bD}. \tag{2}$$

Three parameters were calculated in a voxel-wise approach: coefficient D (mm^2/s), that is, the diffusion coefficient of slow molecular diffusion; coefficient D^* (mm^2/s), that is, the pseudo-diffusion coefficient, reflecting the fast molecular movements associated with flow in the microvasculature or renal tubules; and f, the flowing fraction (%) reflecting all pseudo-randomly flowing water spins in the voxel.

A segmented biexponential fitting approach was followed to reduce computational complexity.[23] Coefficient D was calculated first employing a cutoff b-value of 200 s/mm^2, and thus assuming that pseudo-diffusion can be neglected for values higher than this threshold (i.e., solving the second term of the equation for $f = 0$). Then f and D^* were calculated by fitting the bi-exponential model.

2.4.5 | T1 map

T1 was calculated by fitting, on a voxel-by-voxel basis, the IR data to Equation (3)[14] using the Levenberg-Marquardt algorithm:

$$S_k = M_0 \left(1 - 2e^{-\frac{TI_k}{T1}}\right) + M_0 e^{-\frac{TR}{T1}}, \tag{3}$$

where TI_k is the TI at the kth scan and M_0 is the equilibrium magnetization.

2.4.6 | Kidney segmentation

ROIs were defined to encompass either cortex or medulla solely, as they present different signal behaviors in ASL, IVIM, and T1 data. Cortical and medullary ROIs were manually drawn in the T1 maps and were employed for the PCASL and T1 measurements. For IVIM, cortex and medulla were manually segmented based on the signal intensity changes in the $b = 0$ images. Vascular structures, collecting systems and cysts were excluded from the ROIs. ROI examples are shown in Figure S1, and ROI volumes in Tables S2 and S3.

2.5 | Statistical analysis

Statistical analysis was performed in Python (Python Software Foundation). In all analyses, a p value of less than 0.05 was considered statistically significant. Quantitative variables were expressed as mean (SD) in the ROIs.

Before evaluating the parameters and their correlations with eGFR, data normality was assessed visually looking at the histograms and using Shapiro-Wilk normality tests.

2.5.1 | Reproducibility

To determine intervisit reproducibility and the agreement of mpMRI measures, the within-subject coefficient of variation (CV_{ws}) and intraclass correlation coefficient (ICC) were calculated, and Bland-Altman analysis was performed.

The CV_{ws} (%) was defined as $100 \times (SD/mean)$ with $SD = \sqrt{\left(\sum(x_1 - x_2)^2\right)/2n}$, where x_1 and x_2 are the values of the measured parameters in the two examinations for the same subject, n is the number of subjects, and the mean is the average value over all measurements. The ICC model was chosen to determine the degree of absolute agreement among measurements. Thus a two-way random effects model was employed, the type was single rater, and the definition of the relationship was absolute agreement (form ICC (2,1) according to the Shrout and Fleiss convention).[24]

Finally, to explore the effect of the interval between MRI examinations on the reproducibility results, the CV of MRI parameters was calculated for each subject (as mean divided by SD) and correlations were evaluated between the individual subject CV and the time between MR examinations employing the Spearman correlation coefficient (to allow for a nonlinear relationship).

2.5.2 | Correlation analysis

To understand the relationship among mpMRI parameters and clinical data, an exploratory correlation analysis was performed. Pairwise correlations between parameters themselves and with eGFR were evaluated across the whole study group using the Pearson correlation coefficient. For these analyses, mean parameter values across the two visits in the renal cortex and medulla were employed. For each parameter, outliers were identified according to Tukey's fences criteria and discarded prior to computing the correlation coefficient.

3 | RESULTS

3.1 | Demographic and clinical data

Demographic and clinical data are reported in Table 1. Group mean age was 54 (14) years. Mean time since the transplant was 120 (105) months, and the group average eGFR was 76.89 (13.96) ml/min/1.73m^2. Mean time between visits was 51.67 (44.75) days. In some patients, the time between sessions was higher than originally planned because of the COVID-19 pandemic. In subjects with a time interval between examinations longer than 3 months, it was confirmed that serum creatinine level variation between visits was less than 0.2 mg/g. In two patients, ASL data were not acquired.

3.2 | Labeling efficiency simulations

Measured aortic blood flow velocity profiles are shown in Figure 1A. Peak systolic velocities were significantly higher in Group 1 (96.57 [10.32] cm/s) than in Group 2 (76.89 [12.05] cm/s).

**TABLE 1** Demographic and clinical data of the study patients

#	Age (years)	Sex (M/F)	Donor type	Donor age (years)	Donor sex (M/F)	Time interval since Tx (months)	HTA	DM	Time interval between exams (days)	s-Crea - Exam 1	eGFR[1] - Exam 1	Proteinuria (mg/24 h) - Exam 1	s-Crea - Exam 2	eGFR[1] - Exam 2	Proteinuria (mg/24 h) - Exam 2
1	38	M	cadaveric	59	M	18	Y	N	133	1.60	54	95.70	1.55	56	35.70
2	42	M	cadaveric	44	F	26	Y	N	139	1.10	85	767.60	1.30	70	162.80
3	65	M	cadaveric	68	M	28	Y	N	35	1.30	59	260.80			
4	62	F	living	56	F	70	Y	N	121	0.80	82	163.80	0.80	75	158.40
5	61	M	cadaveric	NA	M	230	Y	N	103	0.81	96	105.60	0.81	96	68.40
6	72	F	cadaveric	NA	NA	389	N	N	97	0.90	69	75.30	1.00	59	136.00
7	39	M	cadaveric	20	M	129	Y	N	26	0.90	113	148.50			
8	36	M	cadaveric	22	M	130	Y	N	14	0.96	88	63.70			
9	59	M	cadaveric	NA	NA	323	N	N	80	0.90	90	1552.50			
10	35	M	living	50	M	99	N	Y	9	1.39	65	145.80			
11	70	F	cadaveric	NA	NA	250	N	N	84	0.92	63	102.50			
12	60	M	living	52	F	51	Y	N	27	1.00	79	75.60			
13	33	F	cadaveric	53	F	26	Y	N	48	1.10	66	196.80			
14	68	F	cadaveric	67	M	39	Y	N	18	0.94	62	850.90			
15	62	M	cadaveric	NA	NA	150	Y	N	17	1.18	66	142.80			
16	60	F	cadaveric	28	M	131	Y	N	7	0.91	69	101.20			
17	64	F	cadaveric	50	F	26	Y	N	9	0.87	70	54.00			
18	28	F	cadaveric	8	NA	196	Y	N	10	0.99	78	70.20			
19	67	M	cadaveric	55	M	61	Y	N	7	0.96	81	210.60			
20	55	F	cadaveric	67	M	37	Y	N	50	0.90	77	237.60			
Mean	53.80	9 F	17 cadaveric	46.60	5F	120.53	4 N	19 N	51.69	1.02	75.60	271.08	1.09	71.20	112.26
SD	13.91	11 M	3 living	17.98	9 M	104.86	16 Y	1 Y	44.75	0.20	13.88	361.68	0.29	14.22	51.05

Abbreviations: CKD-EPI, Chronic Kidney Disease Epidemiology Collaboration; DM, diabetes mellitus; eGFR, estimated glomerular filtration rate; F, female; HTA, hypertension; M, male; N, no; NA, not available; s-Crea, serum creatinine levels; Tx, transplantation; Y, yes.

[1]eGFR was measured with the CKD-EPI creatinine formula in ml/min/1.73m².
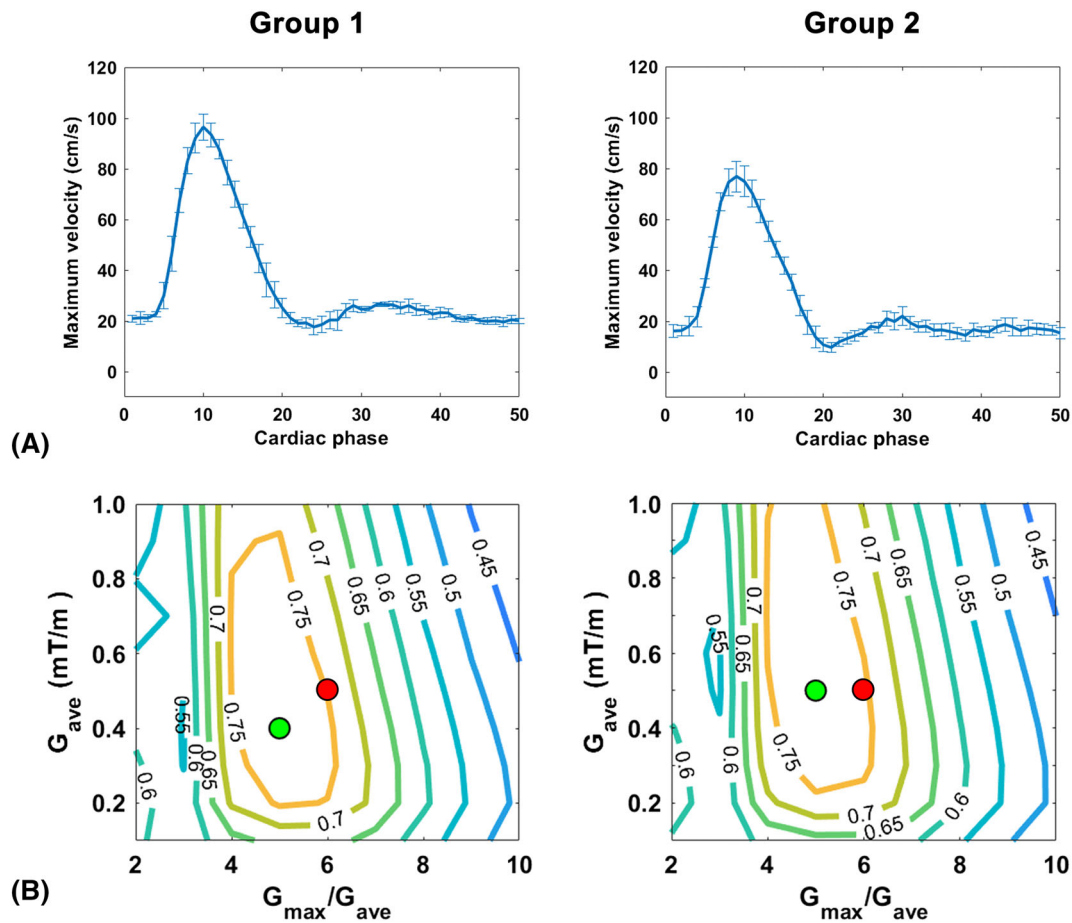
FIGURE 1 (A) Group-averaged blood velocity waveforms measured at the descending aorta for Group 1 (patients aged < 50 years) and Group 2 (patients aged ≥ 50 years). Cross-sectional maximum values are depicted, and the error bars represent the group standard deviation. (B) Simulated labeling efficiency for the two groups. The green circle shows the maximum efficiency value and the red circle shows the efficiency for the employed gradient configuration (G_{max}/G_{ave} ratio of 6 and G_{ave} of 0.5 mT/m)
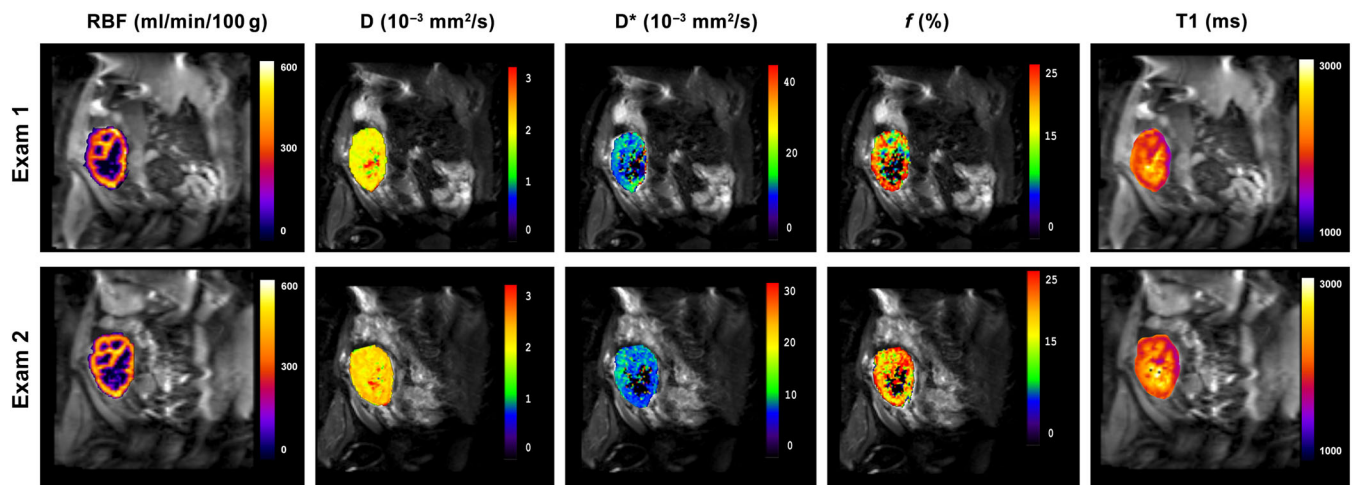
FIGURE 2 Example of multiparametric MRI maps acquired during the two examinations performed on separate days, in a representative patient, showing from left to right: renal blood flow (RBF), diffusion coefficient (D), pseudo-diffusion coefficient (D*), flowing fraction (*f*), and T1

Simulated labeling efficiency maps are displayed in Figure 1B. In Group 1, a maximum efficiency of 79.60% was found at a G_{max}/G_{ave} ratio (R) of 5 and $G_{ave} = 0.4$ mT/m, while in Group 2 it was 79.66% for the same ratio and $G_{ave} = 0.5$ mT/m. Labeling efficiency for the PCASL configuration employed in this study (i.e., R = 6 and $G_{ave} = 0.5$ mT/m) was estimated to be 74.87% for Group 1 and 75.86% for Group 2. The difference

in simulated efficiency between the groups was approximately 1%, indicating that using a single labeling efficiency value for RBF quantification across the whole group was adequate.

3.3 | Multiparametric MRI results

3.3.1 | Allograft perfusion, diffusion, and T1 measurements

In Figure 2, mpMRI maps acquired in a representative subject are illustrated for RBF, D, D*, f, and T1. Quantitative maps obtained in both examinations showed similar values. In Table 2, cortical and medullary parameter values averaged across the group are presented for each examination, and in Figure 3, parameter boxplots are illustrated. For ASL data, TSNR is also reported in Table 2. It can be observed that cortical values were much higher than medullary values for the two examinations. All variables were found to be normally distributed, except for the D* coefficient measured in the first examination in the two compartments.

3.3.2 | Reproducibility results

Bland-Altman plots for cortex and medulla measurements are shown in Figure 4, while CV_{ws} and ICC are displayed in Table 3. The CV_{ws} was very low (< 5%) for T1 and coefficient D in the cortex and medulla, low for cortical RBF (10.73%), and higher for medullary RBF (16.41%), f (cortex: 15.10%, medulla: 18.63%), and coefficient D* (cortex: 15.40%, medulla: 15.69%). Cortical ICC was good for RBF (0.84), moderate for T1 (0.64), flowing fraction f (0.63), and diffusion coefficient D (0.61), and poor for D* (0.15). Medullary ICCs were lower for all the parameters, except for f (0.67) and RBF (0.61), showing poorer reproducibility in this region (T1: 0.47, D: 0.31, and D*: 0.09).

Results of correlation analysis between individual CVs of MRI parameters and time intervals between examinations are shown in Figure S2. It can be observed that only for f there is a trend to higher values as the time interval between examinations increases. Indeed, a significant correlation was found only for f ($p = 0.04$, rho $= 0.49$).

3.3.3 | Correlation analysis

Figure 5 shows the correlation matrix of MRI parameters and eGFR in the cortex and medulla. Correlation coefficients were significant between RBF and f measured in the cortex (r $= 0.66$), between cortical RBF and eGFR (r $= 0.64$), and D* and GFR (r $= -0.57$) (Figure 6). No other significant correlations were found.

TABLE 2 Perfusion, diffusion, and T1 parameters. Values are presented as group mean (SD)

			EXAM 1		EXAM 2		N
PCASL	RBF (ml/min/100 g)	Cortex	196.54	(53.22)	188.35	(49.44)	18
		Medulla	97.30	(22.46)	102.17	(29.37)	18
	PWI (%)	Cortex	2.10	(0.59)	1.99	(0.57)	18
		Medulla	1.04	(0.22)	1.08	(0.29)	18
	TSNR (a.u.)	Cortex	3.61	(1.36)	3.62	(1.19)	18
		Medulla	1.44	(0.65)	1.62	(0.55)	18
IVIM	D (10^{-3} mm²/s)	Cortex	1.93	(0.16)	1.97	(0.15)	20
		Medulla	1.90	(0.12)	1.98	(0.15)	20
	D* (10^{-3} mm²/s)	Cortex	15.59	(2.95)	17.47	(2.26)	20
		Medulla	14.83	(2.64)	24.35	(5.07)	20
	f (%)	Cortex	18.64	(3.70)	16.91	(3.41)	20
		Medulla	16.16	(3.08)	14.38	(3.33)	20
T1 mapping	T1 (ms)	Cortex	1392.11	(99.56)	1372.01	(105.70)	20
		Medulla	1681.12	(60.82)	1641.51	(82.73)	20

Abbreviations: D, diffusion coefficient; D*, pseudo-diffusion coefficient; f, flowing fraction; IVIM, intravoxel incoherent motion; PCASL, Pseudo-Continuous Arterial Spin Labeling; PWI, perfusion-weighted image; RBF, renal blood flow; TSNR, temporal signal-to-noise ratio.
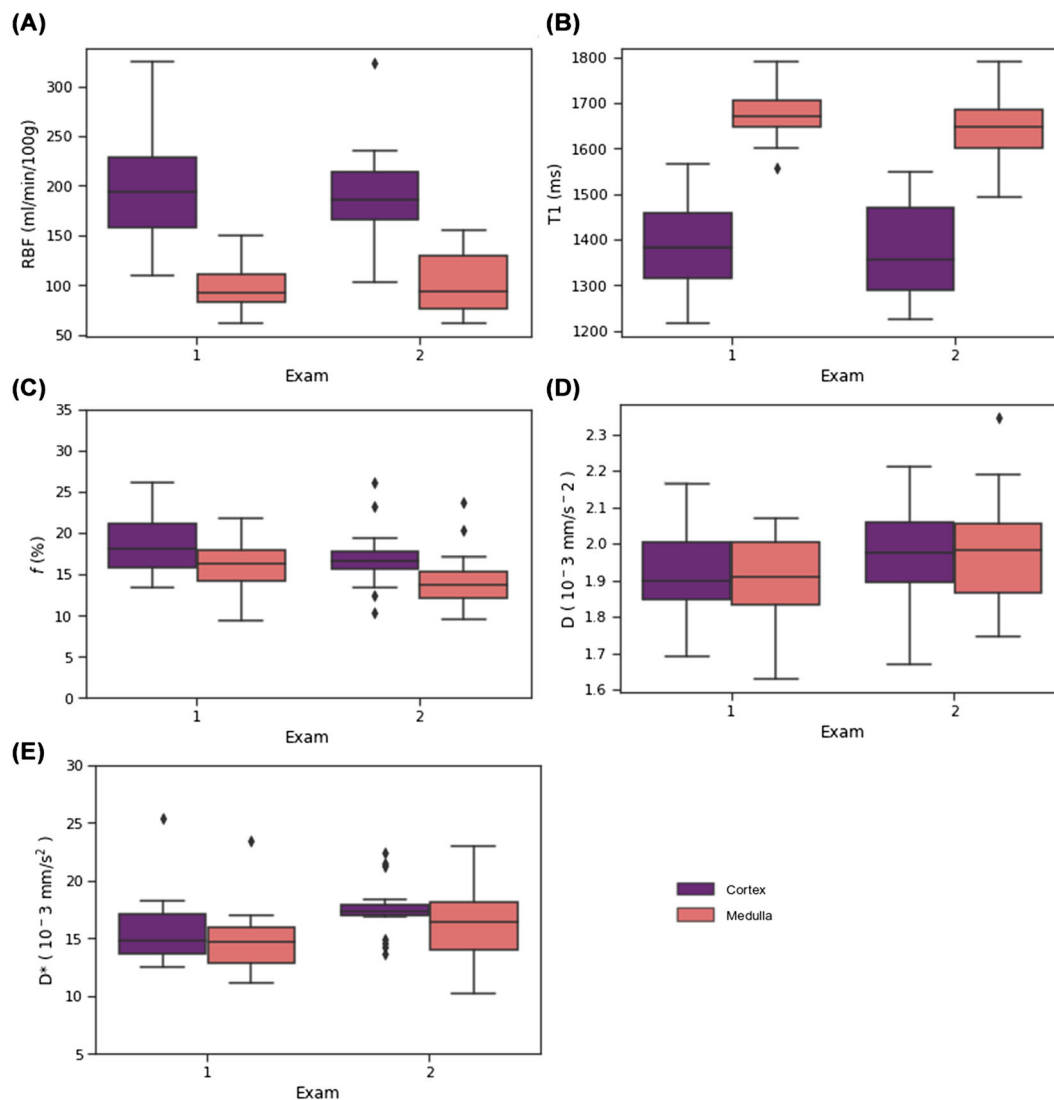
FIGURE 3 Boxplots of cortical (in purple color) and medullary (in salmon color) MRI parameters measured in the two examinations: (A) renal blood flow (RBF), (B) T1 values, (C) flowing fraction (*f*), (D) diffusion coefficient (D), and (E) pseudo-diffusion coefficient (D*)

4 | DISCUSSION

In the current study, a multiparametric MRI protocol was employed in transplant patients with stable renal function with the aims of evaluating reproducibility and assessing the range of normal values of the mpMRI parameters in this group of patients.

Cortical RBF values obtained in this study are in line with values described in the literature, although only a few articles have previously reported RBF in renal allografts measured with PCASL. Yu et al.[25] reported an RBF of 144.73 (49.33) ml/min/100 g in a group of stable patients with a mean eGFR of 72 ml/min/1.73m², using a PCASL 3D-FSE spiral; Wang et al.[26] measured an RBF of 204.7 (44.9) ml/min/100 g in stable patients whose eGFR was 77.1 (15.1) ml/min/1.73m², using a similar PCASL sequence; Rankin et al.[27] showed an RBF of 239 (84) ml/min/100 g measured with PCASL 3D-TGSE in a group of transplant patients with a mean eGFR of 48 ml/min/1.73m² and Ahn et al.[28] obtained an RBF of 358 (36) ml/min/100 g with a PCASL BSSFP sequence employing several postlabeling delays, in a study performed shortly after transplantation.

The variability of the reported RBF measurements is likely due in part to differences in patient characteristics; however, variations in the PCASL sequence implementation and data processing methods can also be a relevant factor. Currently, the major scanner vendors have a body ASL sequence that is available in either a product or a research version. Harmonization of acquisition protocols and data analysis steps following published consensus recommendations[12] will facilitate the comparison of results across scanners.

None of the previously mentioned PCASL studies evaluated the intervisit reproducibility. In our study, an ICC of 0.84 and CV_{ws} of 10.70% were obtained in the cortical region, demonstrating good reproducibility. Medullary RBF presented more variability and reproducibility was lower
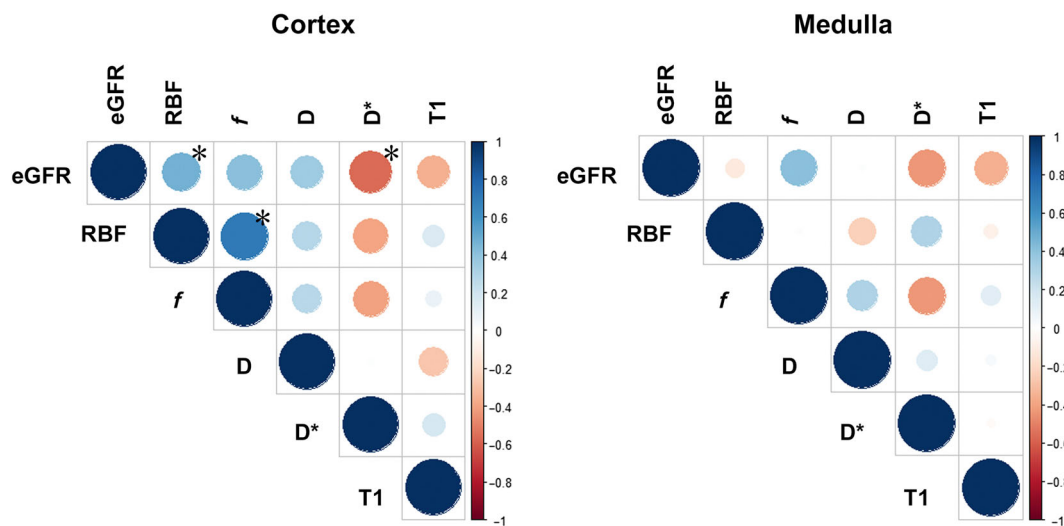
Cortex   Medulla
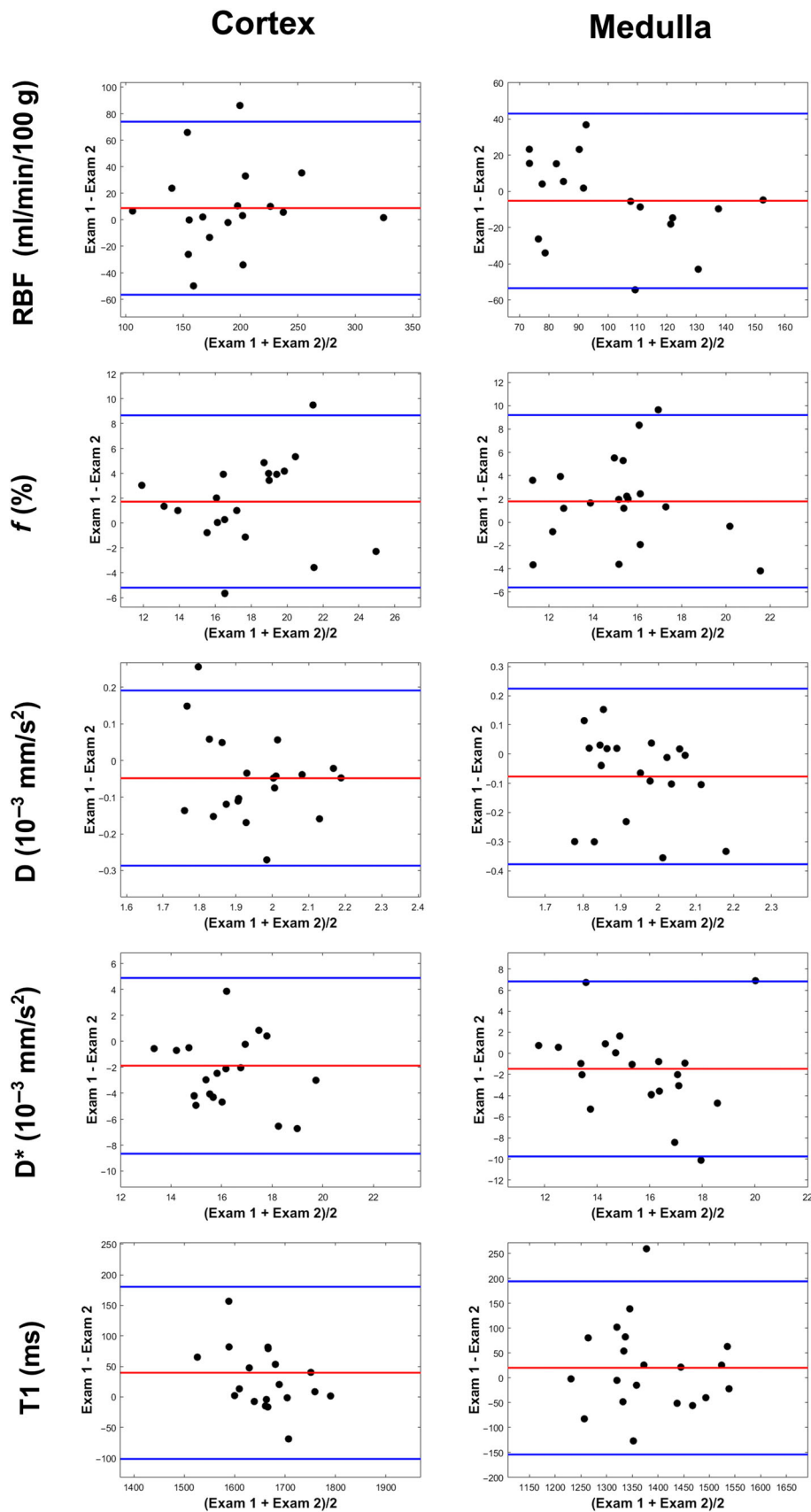
FIGURE 4   Bland-Altman plots of cortical and medullary renal blood flow (RBF), longitudinal relaxation time (T1), flowing fraction (*f*), diffusion coefficient (D), and pseudo-diffusion coefficient (D*) measured in the two examinations. Red and blue lines represent mean difference and limits of agreement (mean ± 2SD)

TABLE 3 Reproducibility results

|				ICC	
			CV$_{ws}$ (%)	ICC	95% CI
PCASL	RBF (ml/min/100 g)	Cortex	10.73%	0.84	[0.64, 0.92]
		Medulla	16.41%	0.61	[0.24, 0.82]
IVIM	D (10^{-3} mm^2/s)	Cortex	4.57%	0.61	[0.26, 0.83]
		Medulla	6.02%	0.31	[−0.04, 0.67]
	D* (10^{-3} mm^2/s)	Cortex	16.26%	0.15	[−0.21, 0.50]
		Medulla	19.54%	0.09	[−0.36, 0.45]
	f (%)	Cortex	15.10%	0.63	[0.08, 0.75]
		Medulla	18.63%	0.67	[−0.09, 0.63]
T1 mapping	T1 (ms)	Cortex	4.46%	0.64	[0.30, 0.84]
		Medulla	3.37%	0.47	[0.07, 0.75]

Abbreviations: CI, confidence interval; CV$_{ws}$, within-subject coefficient of variation; D, diffusion coefficient; D*, pseudo-diffusion coefficient; f, flowing fraction; ICC, intraclass correlation coefficient; IVIM, intravoxel incoherent motion; PCASL, Pseudo-Continuous Arterial Spin Labeling; RBF, renal blood flow.

FIGURE 5 Correlation matrix of multiparametric renal MRI parameters and estimated glomerular filtration rate (eGFR) in the cortex (left) and medulla (right). Positive correlations are displayed in blue, while negative correlations are shown in red. The color intensity and the size of the circle are proportional to the correlation coefficient. D, diffusion coefficient; D*, pseudo-diffusion coefficient; f, flowing fraction; RBF, renal blood flow. *Statistically significant correlation

with a CV$_{ws}$ of 16.41% and ICC of 0.61. The lower medullary reproducibility is likely caused by the low perfusion values and TSNR (which are approximately half those for the cortex) and it could also be affected by the difficulty in differentiating between renal medulla and other tissues in the segmentation. Although reported, medullary RBF measurements do not appear to be as reliable as cortical RBF.

Quantification of perfusion with ASL is affected by variations in the labeling efficiency. PCASL efficiency depends on blood flow velocities in the labeling plane, which are different throughout the aorta and can vary because of age and disease.[21] Because of the location of the transplanted kidney in the iliac fossa, the labeling plane is generally positioned at a lower aortic level than for a native kidney. In this study, aortic blood flow profiles were characterized in kidney transplant patients and employed in simulations to assess the labeling efficiency when locating the labeling plane at this lower position. Velocity waveforms had similar patterns in the two groups of subjects of different ages; however, systolic peak values were 80% lower for the older patients (aged > 50 years). Comparing the velocity waveforms with results from a previous study,[17] in which blood velocity profiles were measured in the supra renal aorta in young healthy volunteers (mean age = 29.7 years), it can be observed that peak velocities in our group of younger patients (mean age = 35.86 years) were lower (91.4 vs. 120 cm/s). These lower values were likely due to the position of the labeling plane in the infrarenal aorta. Peak velocities in the group of older patients were further reduced, confirming the strong effect of age on aortic blood velocities, as previously reported.[17,29]
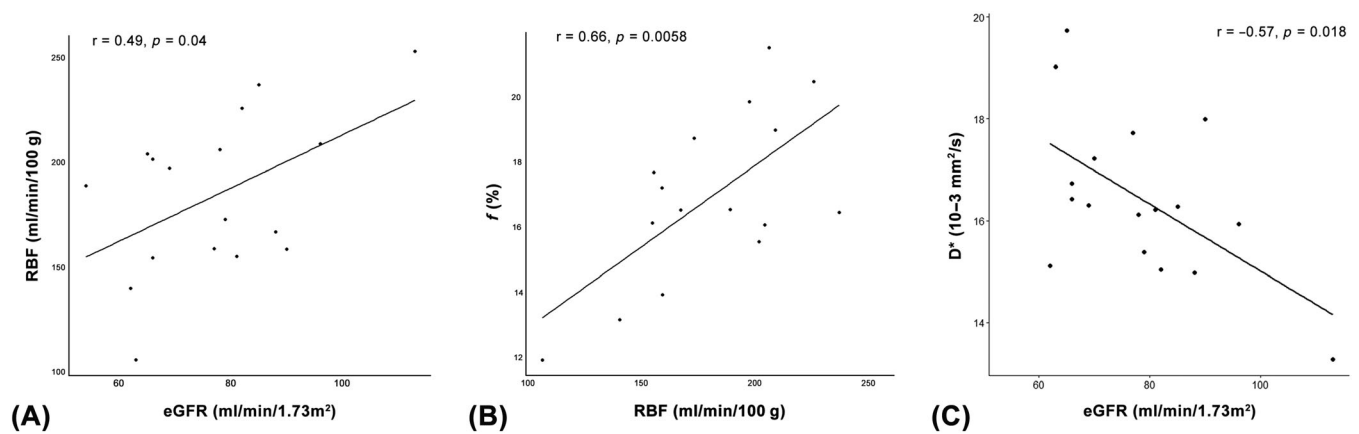
FIGURE 6 Correlations in the cortex between (A) Renal blood flow (RBF) and flowing fraction (*f*) (r = 0.66, p = 0.006), (B) RBF and estimated glomerular filtration rate (eGFR) (r = 0.49 p = 0.04), (C) Pseudo-diffusion coefficient (D*) and eGFR (r = −0.57, p = 0.018)

Field inhomogeneities were also expected at the labeling plane location produced by the different nearby air–tissue and bone–tissue interfaces. These field variations are subject dependent and affect the labeling efficiency, thus simulations included a wide range of off-resonance frequencies. For the gradient parameters employed in the study, the labeling efficiency was ∼75% and the differences between groups were less than 1%, indicating that using a single labeling efficiency value for RBF quantification across the whole group was adequate.

T1 values measured in our cohort of patients showed the expected corticomedullary differentiation, with medullary values being higher than cortical values, as previously reported for both native and transplanted kidneys.[30] T1 measurements on renal transplants are scarce and comparisons across studies are hampered by variations due to field strength and acquisition schemes. Moreover, most studies have been performed in patients early after transplantation, so we cannot directly compare the T1 values measured in this study with results from the literature. Nonetheless, the T1 values reported here are similar to those measured by Friedli et al.[31] in a study including 33 transplant patients, also performed at 3 T, although their study group consisted of a heterogeneous group of patients undergoing a kidney biopsy by clinical indication. Huang et al.[32] measured T1 values in 15 subjects who underwent transplantation from 6 months to 31 years before the MR examination, although eGFR was higher than 60 ml/min/1.73m^2 in only four of them; and more recently, Bane et al.[10] studied patients with stable function over the preceding 3 months with a mean eGFR of 71 ml/min/1.73m^2, a group that is more similar to the one included in our study; however, Bane et al.'s and Huang et al.'s studies were performed at 1.5 T and therefore the T1 values were lower than those reported here, as expected.

Reproducibility of T1 measurements was very high, with a CV$_{ws}$ of ∼4% for both cortex and medulla. This value was lower than previously reported in Bane et al.'s study.[10] The larger number of inversion times employed here probably improved the robustness of the fitting algorithm.

The IVIM parameters D, *f*, and D* measured in this study were in line with reported values in renal allografts with stable kidney function,[10,25,33,34] although there are only a few studies employing IVIM in this group of patients, as the majority of them have studied subjects early after transplantation or allografts with impaired function, and the range of reported values is quite wide.

Thoeny et al.[33] employed IVIM in a group of 15 transplant patients with good kidney function over the previous 3 months. Although data were acquired at 1.5 T, results of D and *f* should be comparable[13] and they are very close to the values measured in our cohort. D* values were not reported by the authors. In the previously mentioned study at 1.5 T, Bane el al.[10] also reported similar values of D, *f*, and D*, while D values measured by Heusch et al.[34] and Yu et al.[25] were slightly lower.

Reproducibility of IVIM parameters was variable, with good results obtained for the diffusion coefficient D, moderate results for *f*, and poor results for D*, both in cortex and medulla, in line with previous works.[10,33] Although the number of b-values in the lower range was larger than in previous studies, this did not translate into improved parameter reproducibility. Increasing the number of b-values further would not be practical as this would increase the acquisition time of the sequence, and that is already quite long. Another strategy to increase reproducibility would be to explore different fitting algorithms, because it has been shown that a Bayesian-based approach decreased the intersubject variability of IVIM parameters.[35]

Good correlation between RBF and *f* was found in this study, as reported previously.[8] Correlation between cortical RBF and eGFR was found to be significant, in agreement with the literature[8,25]; however, the other MRI parameters did not show a significant correlation with eGFR, in contrast to previous reports.[10,32] This could be partly explained by the smaller sample size and the narrow eGFR range in our study compared with other studies, as all the patients were stable with an eGFR of more than 50 ml/min/1.73m^2. Nonetheless, this result suggests that RBF is more closely linked to kidney function than the other MRI parameters, which is consistent with perfusion providing the driving pressure for glomerular filtration.

Because of the allograft location in the iliac fossa, the MRI protocol could be performed in free breathing, simplifying the acquisition, and not exceeding the protocol duration of 30 min. In ASL, in which perfusion is calculated as the signal difference between two images, voxel correspondence is critically important. Although slight in-plane motion was detected throughout the image time series, it was successfully corrected during postprocessing. In addition, background suppression pulses were employed to remove background signal and minimize subtraction errors. In the case of diffusion and T1 mapping data, motion effects were also corrected during postprocessing.

4.1 | Limitations

The main limitation of this study was the sample size, which was relatively small, although this was partly compensated by the homogeneity of the study group. Further studies in larger groups of patients with stable function will help to better characterize perfusion, diffusion, and T1 values in this cohort.

Although IVIM-derived f and ASL-derived RBF cortical data correlated well, a bias in the ROIs could not be excluded as two manual ROIs were drawn for the two sets of images according to their resolution and readout. This could be improved by performing intersequence registration followed by automated ROI segmentation.

The different ROI volumes across patients could be considered another shortcoming. ROI volumes were dependent on allograft size, characteristics (e.g., in kidneys with cysts the ROI volumes were reduced), and orientation, which in some cases prevented the acquisition of the images along the long axis of the kidney.

Finally, another limitation of this work is the heterogeneity in the time interval between the two MRI examinations, which could have affected the reproducibility measurements. However, the patients included were categorized by the referring nephrologist as clinically stable, based on serum creatinine measurements obtained in the year prior to their inclusion, and no patients experienced any adverse event that changed their clinical status during the period between the two examinations, thus it is reasonable to assume that their renal function and structure did not vary during this time. Moreover, correlations between the variability of MRI parameters (as measured by the individual CV) and the time interval between examinations were not found, except in the case of the flowing fraction (f).

4.2 | Conclusion

In the current study, the reproducibility of performing a mpMRI protocol in kidney transplant patients with stable function was evaluated. This abbreviated protocol, employing three sequences, followed recommended implementations by expert panels,[12–14] and normal values of the measured parameters in this group of patients were characterized, enabling comparisons with future studies. The results showed good reproducibility of the techniques in the renal cortex, supporting their potential for clinical applicability.

CONFLICTS OF INTEREST
The authors declare no conflict of interest. Marta Vidorreta is an employee of Siemens Healthcare Spain.

ORCID
Rebeca Echeverria-Chasco 🔟 https://orcid.org/0000-0003-0199-2593

REFERENCES
1. Hill NR, Fatoba ST, Oke JL, et al. Global prevalence of chronic kidney disease – A systematic review and meta-analysis. *PLoS One.* 2016;11(7): e0158765. doi:10.1371/journal.pone.0158765
2. Loupy A, Aubert O, Orandi BJ, et al. Prediction system for risk of allograft loss in patients receiving kidney transplants: international derivation and validation study. *BMJ.* 2019;366:1-12. doi:10.1136/bmj.l4923
3. Kasiske BL, Zeier MG, Chapman JR, et al. Kidney disease: improving global outcomes. KDIGO clinical practice guideline for the care of kidney transplant recipients: A summary. *Kidney Int.* 2010;77(4):299-311. doi:10.1038/ki.2009.377
4. Porrini E, Ruggenenti P, Luis-Lima S, et al. Estimated GFR: time for a critical appraisal. *Nat Rev Nephrol.* 2019;15(3):177-190. doi:10.1038/s41581-018-0080-9
5. Heaf JG, Iversen J. Uses and limitations of renal scintigraphy in renal transplantation monitoring. *Eur J Nucl Med.* 2000;27(7):871-879. doi:10.1007/s002590000281

6. Jehn U, Schuette-Nuetgen K, Kentrup D, Hoerr V, Reuter S. Renal allograft rejection: noninvasive ultrasound- and MRI-based diagnostics. *Contrast Media Mol Imaging*. 2019;9:3568067. doi:10.1155/2019/3568067

7. Selby NM, Blankestijn PJ, Boor P, et al. Magnetic resonance imaging biomarkers for chronic kidney disease: a position paper from the European Cooperation in Science and Technology Action PARENCHIMA. *Nephrol Dial Transplant*. 2018;33(Suppl. 2):4-14. doi:10.1093/ndt/gfy152

8. Heusch P, Wittsack HJ, Heusner T, et al. Correlation of biexponential diffusion parameters with arterial spin-labeling perfusion MRI: Results in transplanted kidneys. *Invest Radiol*. 2013;48(3):140-144. doi:10.1097/RLI.0b013e318277bfe3

9. Ren T, Wen C-LL, Chen L-HH, et al. Evaluation of renal allografts function early after transplantation using intravoxel incoherent motion and arterial spin labeling MRI. *Magn Reson Imaging*. 2016;34(7):908-914. doi:10.1016/j.mri.2016.04.022

10. Bane O, Hectors SJ, Gordic S, et al. Multiparametric magnetic resonance imaging shows promising results to assess renal transplant dysfunction with fibrosis. *Kidney Int*. 2020;97(2):414-420. doi:10.1016/j.kint.2019.09.030

11. Adams LC, Bressem KK, Scheibl S, et al. Multiparametric assessment of changes in renal tissue after kidney transplantation with quantitative MR relaxometry and diffusion-tensor imaging at 3 T. *J Clin Med*. 2020;9(5):1-16. doi:10.3390/jcm9051551

12. Nery F, Buchanan CE, Harteveld AA, et al. Consensus-based technical recommendations for clinical translation of renal ASL MRI. *Magn Reson Mater Physics, Biol Med*. 2020;33(1):141-161. doi:10.1007/s10334-019-00800-z

13. Ljimani A, Caroli A, Laustsen C, et al. Consensus-based technical recommendations for clinical translation of renal diffusion-weighted MRI. *Magn Reson Mater Physics, Biol Med*. 2020;33(1):177-195. doi:10.1007/s10334-019-00790-y

14. Dekkers IA, de Boer A, Sharma K, et al. Consensus-based technical recommendations for clinical translation of renal T1 and T2 mapping MRI. *Magn Reson Mater Physics, Biol Med*. 2020;33(1):163-176. doi:10.1007/s10334-019-00797-5

15. Schieda N, Blaichman JI, Costa AF, Glikstein R, Hurrell C, James M. Gadolinium-based contrast agents in kidney disease: A comprehensive review and clinical practice guideline issued by the Canadian Association of Radiologists. *Can J Kidney Health Dis*. 2018;5:2054358118778573. doi:10.1177/2054358118778573

16. Levey AS, Stevens LA, Schmid CH, et al. A new equation to estimate glomerular filtration rate. *Ann Intern Med*. 2009;150(9):604-612. doi:10.7326/0003-4819-150-9-200905050-00006

17. Echeverria-Chasco R, Vidorreta M, Aramendía-Vidaurreta V, et al. Optimization of pseudo-continuous arterial spin labeling for renal perfusion imaging. *Magn Reson Med*. 2020;85(3):1507-1521. doi:10.1002/mrm.28531

18. Taso M, Guidon A, Alsop DC. Influence of background suppression and retrospective realignment on free-breathing renal perfusion measurement using pseudo-continuous ASL. *Magn Reson Med*. 2019;81(4):2439-2449. doi:10.1002/mrm.27575

19. Huizinga W, Poot DHJ, Guyader JM, et al. PCA-based groupwise image registration for quantitative MRI. *Med Image Anal*. 2016;29:65-78. doi:10.1016/j.media.2015.12.004

20. Klein S, Staring M, Murphy K, Viergever MA, Pluim JPW. elastix: a toolbox for intensity-based medical image registration. *IEEE Trans Med Imaging*. 2010;29(1):196-205. doi:10.1109/TMI.2009.2035616

21. Garcia J, van der Palen RLF, Bollache E, et al. Distribution of blood flow velocity in the normal aorta: Effect of age and gender. *J Magn Reson Imaging*. 2018;47(2):487-498. doi:10.1002/jmri.25773

22. Maccotta L, Detre JA, Alsop DC. The efficiency of adiabatic inversion for perfusion imaging by arterial spin labeling. *NMR Biomed*. 1997;10(4-5):216-221. doi:10.1002/(SICI)1099-1492(199706/08)10:4/53.0.CO;2-U

23. Jalnefjord O, Andersson M, Montelius M, Starck G, Karin A, Viktor E. Comparison of methods for estimation of the intravoxel incoherent motion (IVIM) diffusion coefficient (D) and perfusion fraction (f). *Magn Reson Mater Physics, Biol Med*. 2018;31(6):715-723. doi:10.1007/s10334-018-0697-5

24. McGraw KO, Wong SP. Forming inferences about some intraclass correlation coefficients. *Psychol Methods*. 1996;1(1):30-46. doi:10.1037/1082-989X.1.1.30

25. Yu YM, Wang W, Wen J, Zhang Y, Lu GM, Zhang LJ. Detection of renal allograft fibrosis with MRI: arterial spin labeling outperforms reduced field-of-view IVIM. *Eur Radiol*. 2021;31(9):6696-6707. doi:10.1007/s00330-021-07818-9

26. Wang Y, Li Y, Yin L, Pu H, Chen J-Y. Functional assessment of transplanted kidneys with magnetic resonance imaging. *World J Radiol*. 2015;7(10):343-349. doi:10.4329/wjr.v7.i10.343

27. Rankin AJ, Allwood-Spiers S, Lee MMY, et al. Comparing the interobserver reproducibility of different regions of interest on multi-parametric renal magnetic resonance imaging in healthy volunteers, patients with heart failure and renal transplant recipients. *Magn Reson Mater Physics, Biol Med*. 2020;33(1):103-112. doi:10.1007/s10334-019-00809-4

28. Ahn HS, Yu HC, Kwak HS, Park SH. Assessment of renal perfusion in transplanted kidney patients using pseudo-continuous arterial spin labeling with multiple post-labeling delays. *Eur J Radiol*. 2020;130(July):109200. doi:10.1016/j.ejrad.2020.109200

29. Van Ooij P, Garcia J, Potters WV, et al. Age-related changes in aortic 3D blood flow velocities and wall shear stress: Implications for the identification of altered hemodynamics in patients with aortic valve disease. *J Magn Reson Imaging*. 2016;43(5):1239-1249. doi:10.1002/jmri.25081

30. Wolf M, de Boer A, Sharma K, et al. Magnetic resonance imaging T1- and T2-mapping to assess renal structure and function: a systematic review and statement paper. *Nephrol Dial Transplant*. 2018;33(suppl_2):ii41-ii50. doi:10.1093/ndt/gfy198

31. Friedli I, Crowe LA, Berchtold L, et al. New magnetic resonance imaging index for renal fibrosis assessment: A comparison between diffusion-weighted imaging and T1 mapping with histological validation. *Sci Rep*. 2016;6(June):1-15. doi:10.1038/srep30088

32. Huang Y, Sadowski EA, Artz NS, et al. Measurement and comparison of T1 relaxation times in native and transplanted kidney cortex and medulla. *J Magn Reson Imaging*. 2011;33(5):1241-1247. doi:10.1002/jmri.22543

33. Thoeny HC, Zumstein D, Simon-Zoula S, et al. Functional evaluation of transplanted kidneys with diffusion-weighted and BOLD MR imaging: initial experience. *Radiology*. 2006;241(3):812-821. doi:10.1148/radiol.2413060103

34. Heusch P, Wittsack H-J, Pentang G, et al. Biexponential analysis of diffusion-weighted imaging: comparison of three different calculation methods in transplanted kidneys. *Acta Radiol*. 2013;54(10):1210-1217. doi:10.1177/0284185113491090

35. Barbieri S, Donati OF, Froehlich JM, Thoeny HC. Impact of the calculation algorithm on biexponential fitting of diffusion-weighted MRI in upper abdominal organs. *Magn Reson Med*. 2016;75(5):2175-2184. doi:10.1002/mrm.25765

SUPPORTING INFORMATION

Additional supporting information can be found online in the Supporting Information section at the end of this article.